Semicond. Sci. Technol. **13** (1998) 871–875. Printed in the UK PII: S0268-1242(98)91385-2

# Exciton and confinement potential effects on the resonant Raman scattering in quantum dots

**E Menéndez-Proupin†‡, J L Peña†§ and C Trallero-Giner‡**

† Centro de Investigación y Estudios Avanzados del Instituto Politécnico Nacional, Unidad Mérida, A.P. 73 'Cordemex', C.P. 97310, Mérida, Yucatán, Mexico
‡ Universidad de La Habana, Dept de Física Teórica, Vedado 10400, La Habana, Cuba
§ Centro de Investigación en Ciencia Aplicada y Technología Avanzada del Instituto Politécnico Nacional, Legaria 694, C.P.11500, México

Received 5 February 1998, in final form 21 April 1998, accepted for publication 20 May 1998

**Abstract.** Resonant Raman scattering in spherical semiconductor quantum dots is theoretically investigated. The Fröhlich-like interaction between electronic states and optical vibrations has been considered. The Raman profiles are studied for the following intermediate electronic state models: (I) uncorrelated electron–hole pairs in the strongly size-dependent quantized regime; (II) Wannier–Mott excitons in an infinite potential well; (III) excitons in a finite confinement barrier. It is shown that the finite confinement barrier height and the electron–hole correlation determine the absolute values of the scattering intensities and substantially modify the Raman lineshape, even in the strong confinement regime.

## 1. Introduction

During the last decade, technological developments have made possible the fabrication of one- and zero-dimensional nanostructures such as quantum wires and quantum dots (QDs). The interest in these systems comes from their novel optical and transport properties and has been stimulated by the success of quantum wells in technology. The effect of reduced dimensionality on the electronic excitations and the related optical properties has been the subject of intensive investigation and nowadays it is more or less wellunderstood.

Semiconductor-doped glasses (SDGs) are particularly useful to investigate the vibrational modes in quasi-zero-dimensional systems, because the use of appropriate thermal annealing techniques makes it possible to grow semiconductor nanocrystallites with small enough radius to show the effects of spatial confinement on the optical vibrational modes. Raman spectroscopy is a valuable tool to probe the active optical modes and also to obtain information about the electronic system. In addition, resonant Raman scattering (RRS) can be used as a size selective technique [1], which could play an important role on SDGs due to their broad dispersion in microcrystallite sizes. Recently, the mechanism and features of Raman scattering by semiconductor nanocrystallites have been studied [2–5], showing the effects of the reduced dimensionality on the Raman shift and lineshape. A preliminary theory of first-order RRS in spherical microcrystallites has been developed in [2] and [6] on the basis of a continuum model for polar optical vibrations. These models consider the electronic intermediate states as uncorrelated electron–hole pair (EHP) states, that is, in the strong size quantized regime (model I). An extension to the above theories, considering the electron–hole interaction effects, has been recently presented [7] (model II). The calculations performed in [7] are strictly valid for excitons completely confined within dots. Raman scattering in the Fröhlich configuration considerably depends on the differences between electron and hole wavefunctions (*electron–hole decompensation*) [8]. The theoretical values of the Raman cross-section and lineshape should be modified by the electron–hole model and the confinement potential used in the entire calculation. Hence, in the framework of a free EHP model with infinite barriers the same wavefunctions for electrons and holes are obtained and null contribution of the Fröhlich mechanism to the Raman cross-section is achieved. The scattering efficiencies following models I and II considerably differ when absolute values are calculated, even for QDs with radii smaller than the exciton Bohr radius. In model I the finite confinement barriers are considered but regardless of excitonic effects. Model II includes the electron–hole correlation in an infinite barrier, but the chosen potential diminishes the electron–hole decompensation occurring through the finite band offsets potential. In [7] on the lines of model II an effective radius $R_{ef}$ was introduced in order to take into account the penetration of the exciton

0268-1242/98/080871+05$19.50 © 1998 IOP Publishing Ltd 

wavefunction into the adjacent medium. This procedure allows, in some way, the RRS calculations in real systems using the mathematical simplicity of the infinite-barrier basis functions. We will show that within the above approach accurate exciton ground-state energies can be achieved but this approach underestimates the calculated Raman absolute values. It is well established that a reliable Raman scattering theory becomes necessary in order to interpret RRS absolute values in semiconductors [9]. The purpose of the present paper is to clarify the electron–hole decompensation effect on the absolute values of scattering intensities and Raman lineshapes, taking into account uncorrelated and correlated electron–hole theories and using different confinement potential models.

The paper is organized as follows. In section 2 we provide the theoretical basis needed to obtain the Raman cross-section where the electronic intermediate states are excitons in a finite spherical potential box (model III). Theories I and II are derived as proper limits from the more general model III. We also compare the Raman intensity values for CdS QDs embedded in a glass matrix, obtained along the lines of the above-described theoretical models. In section 3 we present the conclusions of the present work.

## 2. Results and discussion

The Raman cross-section $\partial^2\sigma/\partial\Omega\partial\omega_s$ of a dot of radius $R$ can be expressed as [7]

$$\frac{\partial^2\sigma}{\partial\Omega\partial\omega_s} = S_0 \times\sum_{n_p}\left|\sum_{N,N'}\frac{f_N\langle N|h_{E-P}^{(n_p)}|N'\rangle f_{N'}}{(\hbar\omega_s - E_{N'}(R)+\mathrm{i}\Gamma_{N'})(\hbar\omega_l - E_N(R)+\mathrm{i}\Gamma_N)}\right|^2 \times\frac{\Gamma_{n_p}/\pi}{(\hbar\omega_l-\hbar\omega_s-\hbar\omega_{n_p}(R))^2+\Gamma_{n_p}^2}. \quad (1)$$

Here, $\hbar\omega_l$ ($\hbar\omega_s$) is the incoming (outgoing) photon energy, $E_N$ ($\Gamma_N$) is the energy (broadening) of the intermediate $L=0$ electronic state $|N\rangle$ ($L$ being the quantum number of the total electronic angular momentum squared), $f_N$ their optical strengths, $\langle N|h_{E-P}^{(n_p)}|N'\rangle$ is the matrix element of the electron–Fröhlich-type lattice interaction (in dimensionless units [7]) and $n_p$ is the vibron [10] quantum number with angular momentum $l_p=0$ and frequency $\omega_{n_p}$. $S_0$ is a constant which depends on the semiconductor parameters and the embedding medium [7].

The exciton wavefunction $\Psi(\boldsymbol{r}_e,\boldsymbol{r}_h)$ is obtained by the expansion

$$\Psi_{N,L,M}(\boldsymbol{r}_e,\boldsymbol{r}_h) = \sum_{\alpha=\{n_e,n_h,l_e,l_h\}} C_{N,L,M}(\alpha)\Phi_\alpha(\boldsymbol{r}_e,\boldsymbol{r}_h) \quad (2)$$

where the basis functions $\Phi_\alpha(\boldsymbol{r}_e,\boldsymbol{r}_h)$ are eigenfunctions of the total angular momentum squared $\hat{L}^2$, its $z$ projection $\hat{L}_z$ and the Hamiltonian of the free EHP in the dot. The functions $\Phi_\alpha(\boldsymbol{r}_e,\boldsymbol{r}_h)$ are constructed from the dot electron and hole wavefunctions ($\phi_{n_e,l_e,m_e}(\boldsymbol{r}_e)$ and $\phi_{n_h,l_h,m_h}(\boldsymbol{r}_h)$), through the relation

$$\Phi_\alpha(\boldsymbol{r}_e,\boldsymbol{r}_h) = \sum_{m_e,m_h}(l_e l_h m_e m_h|LM)\phi_{n_e,l_e,m_e}(\boldsymbol{r}_e)\phi_{n_h,l_h,m_h}(\boldsymbol{r}_h) \quad (3)$$

($l_e l_h m_e m_h|LM$) being the well known Clebsch–Gordan coefficients.

The coefficients $C_{N,L,M}(\alpha)$ and the eigenenergy $E_N$ are obtained from numerical diagonalization of the exciton Hamiltonian in a spherical potential well, using the basis defined by equation (3) [11]. If the uncorrelated theory (model I) is considered, for every eigenstate there is only one non-zero coefficient $C_{N,L,M}(\alpha)$ in the expansion (2). This approach leads to the same results as the formalism of [6]. On the other hand, models II and III differ upon the radial parts of the electronic wavefunctions $\phi_{n_e,l_e,m_e}(\boldsymbol{r}_e)$ and $\phi_{n_h,l_h,m_h}(\boldsymbol{r}_h)$, which depend on the chosen confinement potential.

The resonance condition with a particular electronic level $N$ is given by the equations $\hbar\omega_s = E_N(R)$ (outgoing resonance) or $\hbar\omega_l = E_N(R)$ (incoming resonance). In the dipole approximation only excitons with $L=0$ are created or annihilated, corresponding to $l_e = l_h$ interband transitions in the free EHP model. If the valence-band mixing is neglected, only $l_p = 0$ vibrons contribute to the Raman scattering.

The calculation of the matrix elements of equation (1) has been performed in [7] for the case of totally confined excitons, while the strong size quantized regime (non-exciton effects) has been developed in [6]. The parameters used in our calculations correspond to a CdS QD of radius 20 Å [7]. This means that the dot is in the strong confinement regime. In this regime the Coulomb attraction shifts the EHP energies to lower values and small changes in the wavefunctions are expected.

Figure 1 shows the electron and hole density of probability for the three lower $L=0$ excitonic eigenstates as functions of $r$, the distance to the dot centre. The density of probability in the case of the uncorrelated EHP model (I) is shown by a dashed curve. For the $N=1$, $L=0$ excitonic state the effect of the correlation is to push both the electron and the hole to the dot centre. As can be seen, for the system under consideration (CdS QD of radius 20 Å) the effect of the finite confinement on the electron–hole decompensation is larger than that of the electron–hole interaction. As we shall see, if the former effect is neglected considerable changes in the predicted Raman cross-section absolute values are obtained. In figure 2(a) we compare the calculated Raman cross-section for incoming light in resonance with the $N=1$ excitonic state following models I, II and III. The incoming resonances happen at $\hbar\omega_l = 2.870$ eV in the finite-barrier excitonic model III (solid curve), at $\hbar\omega_l = 3.014$ eV in the uncorrelated EHP model I (dashed curve) and at $\hbar\omega_l = 2.878$ eV for the excitonic model II (dot-dashed curve), assuming an effective radius $R_{ef} = 26$ Å to simulate the finite-barrier height. It can be seen that accurate $N=1$ exciton energy can be obtained following the formalism of model II. The $N=1$ excitonic state, as can be seen in table 1(a), is mainly composed of EHP states with quantum numbers $n_e = n_h = 1$, $l_e = l_h = 0$ with a large oscillator strength $|f_N|^2$, giving the main contribution to the cross-section in the resonance condition. The lineshape is almost the same in the three models. The difference between those models lies in the absolute values of the cross-section, which is

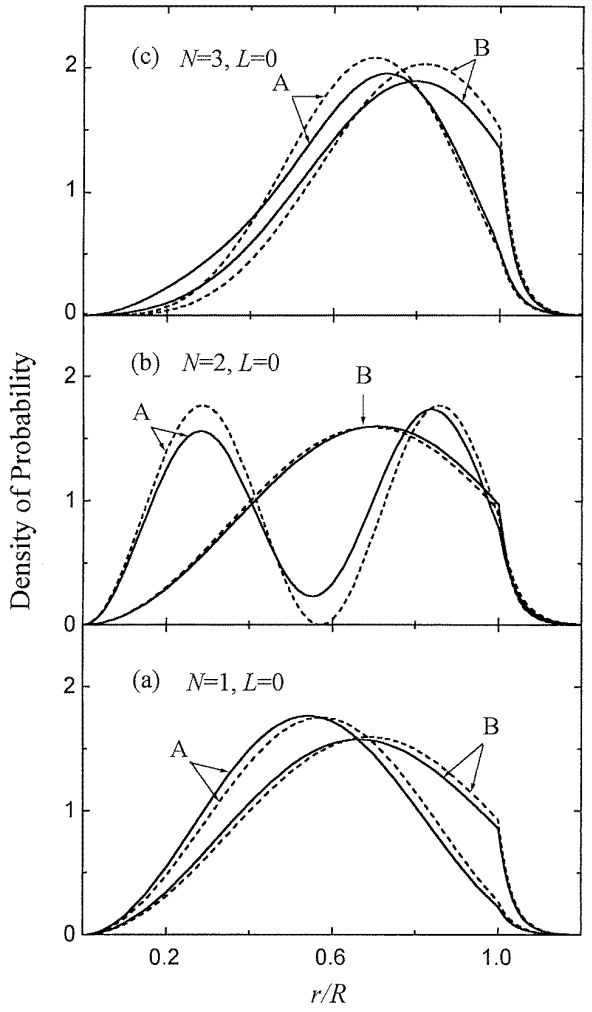


**Figure 1.** Density of probability function for the hole (curve A) $4\pi r^2 \int |\Psi_N(\boldsymbol{r}_e, \boldsymbol{r})|^2 \, \mathrm{d}^3\boldsymbol{r}_e$ and for the electron (curve B) $4\pi r^2 \int |\Psi_N(\boldsymbol{r}, \boldsymbol{r}_h)|^2 \, \mathrm{d}^3\boldsymbol{r}_h$, for the states $N = 1, 2, 3$ and $L = 0$ considering finite band offsets. The solid curves correspond to calculations using the excitonic model and the dashed curves, using the free electron–hole pair model.

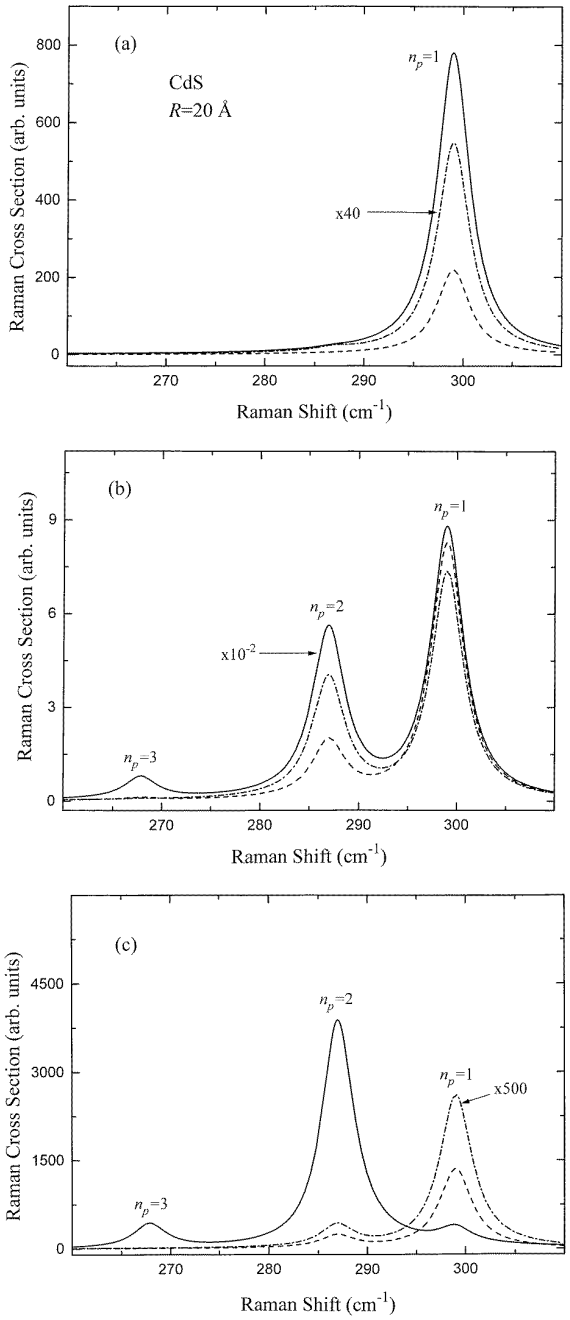


**Figure 2.** Raman cross-section of a 20 Å CdS quantum dot, calculated using different electronic models: (I) uncorrelated EHP intermediate states (dashed curve); (II) excitonic intermediate states in a spherical box with an effective radius $R_{ef}$ = 26 Å (dot-dashed curve); (III) excitonic intermediate states (solid curve). (a) At $\hbar\omega_l$ = 3.014, 2.878 and 2.870 eV for models I, II and III respectively (incoming resonance with $N = 1$, $L = 0$ EHP); (b) at $\hbar\omega_l$ = 3.439, 3.205 and 3.292 eV for models I, II and III respectively (incoming resonance with $N = 2$, $L = 0$ EHP); (c) at $\hbar\omega_l$ = 3.479, 3.310 and 3.339 eV for models I, II and III respectively (incoming resonance with $N = 3$, $L = 0$ EHP).

smaller in model II. It is clear that the dominant effect on absolute values comes from: (a) the values of the oscillator strength [12]; (b) the EHP wavefunctions decompensation produced by the finite depth of the spherical well. It can be seen from figure 1 that the electron–hole decompensation for the first level is slightly larger in model III than the free EHP theory (I), something that is reflected in the values of the exciton–vibron matrix elements reported in table 1. In the case of excitons completely confined (II) the exciton–vibron matrix elements $\langle 1|h^{(n_p)}|1\rangle$ are one order of magnitude smaller than I and III (see [7]). However, we must note that in the case of the electrons, the effective mass in the glass matrix is five times larger than its value inside the dot, causing an extremely large decompensation. A similarly large effect can be achieved if one of the barrier heights is too small.

Figure 2(b) shows the Raman spectrum in the case of incoming resonance with the $N = 2$ exciton at $\hbar\omega_l = 3.439$, 3.205 and 3.292 eV in models I, II and III respectively. In I, the $N = 2$ state is the free EHP with quantum numbers $n_e = 1, n_h = 2, l_e = l_h = 0$ and it has a weak optical activity, as can be seen from the corresponding oscillator strength

**Table 1.** Values of the coefficients $C_{N,0,0}$, resonance energies $E_N$ (incoming) and $E_N + \hbar\omega_p$ (outgoing), oscillator strength $|f_N|^2$ and dimensionless exciton-lattice matrix elements $\langle N|h_{E-P}^{(n_p)}|N'\rangle$ for different $n_p$ vibronic modes contributing to the Raman cross-section, calculated using the excitonic and the free electron–hole pair models with finite barriers and the parameters of [7].

| $N$ | $C_{N,0,0}(n_e, n_h, l_e, l_h)^2$ | $E_N$ (eV) ($E_N + \hbar\omega_p$) | $\lvert f_N\rvert^2$ | $n_p$ | $\langle N\lvert h_{E-P}^{(n_p)}\rvert N\rangle$ | $\langle N\lvert h_{E-P}^{(n_p)}\rvert N+1\rangle$ |
|---|---|---|---|---|---|---|
| (a) Excitonic model | | | | | | |
| | | 2.870 | | 1 | $-9.5 \times 10^{-2}$ | $2.3 \times 10^{-1}$ |
| 1 | $C(1,1,0,0)^2 = 0.98$ | (2.908) | 1.67 | 2 | $-8.4 \times 10^{-3}$ | $9.4 \times 10^{-2}$ |
| | | | | 3 | $-8.1 \times 10^{-5}$ | $-1.3 \times 10^{-3}$ |
| | $C(1,2,0,0)^2 = 0.83$ | 3.292 | | 1 | $-1.1 \times 10^{-1}$ | $3.8 \times 10^{-3}$ |
| 2 | $C(1,1,1,1)^2 = 0.16$ | (3.329) | 1.08 | 2 | $-1.4 \times 10^{-1}$ | $-6.2 \times 10^{-2}$ |
| | | | | 3 | $-5.0 \times 10^{-2}$ | $-1.8 \times 10^{-2}$ |
| | $C(1,2,0,0)^2 = 0.16$ | 3.339 | | 1 | $-5.9 \times 10^{-2}$ | $-1.1 \times 10^{-1}$ |
| 3 | $C(1,1,1,1)^2 = 0.82$ | (3.376) | 2.74 | 2 | $4.0 \times 10^{-3}$ | $4.2 \times 10^{-3}$ |
| | | | | 3 | $8.3 \times 10^{-3}$ | $2.1 \times 10^{-2}$ |
| (b) Free electron–hole pair model | | | | | | |
| | | 3.014 | | 1 | $-8.6 \times 10^{-2}$ | $-2.6 \times 10^{-1}$ |
| 1 | $C(1,1,0,0)^2 = 1$ | (3.051) | 0.96 | 2 | $-3.0 \times 10^{-3}$ | $-9.2 \times 10^{-2}$ |
| | | | | 3 | $-2.8 \times 10^{-4}$ | $-5.3 \times 10^{-3}$ |
| | | 3.439 | | 1 | $-1.2 \times 10^{-1}$ | 0 |
| 2 | $C(1,2,0,0)^2 = 1$ | (3.476) | 0.03 | 2 | $-1.7 \times 10^{-1}$ | 0 |
| | | | | 3 | $-5.0 \times 10^{-2}$ | 0 |
| | | 3.479 | | 1 | $-7.0 \times 10^{-2}$ | 0 |
| 3 | $C(1,1,1,1)^2 = 1$ | (3.516) | 2.87 | 2 | $2.6 \times 10^{-2}$ | 0 |
| | | | | 3 | $-1.9 \times 10^{-3}$ | 0 |

$|f_N|^2$ in table 1(b). Nevertheless, the excitonic effects produced by the Coulomb interaction greatly enhance its oscillator strength (see table 1(a)) and a strong incoming resonance is obtained. It must be noted that even when the matrix element $\langle 2|h^{(n_p)}|2\rangle$ is maximum for $n_p = 2$, the main contribution to the cross-section in figure 2(b) corresponds to $n_p = 1$, a fact that can be explained by interference effects due to virtual transitions between $N = 2$ and $N = 3$ excitonic levels. Figure 1(b) shows that electron–hole decompensation is similar for I and III. Nevertheless a completely confined exciton theory with an effective radius gives matrix elements $\langle 2|h^{(n_p)}|2\rangle$ one order of magnitude smaller than those reported in table 1.

Figure 2(c) shows the spectrum for the case of incoming resonance with the $N = 3$ level, at $\hbar\omega_l = 3.479$, 3.310 and 3.339 eV in models I, II and III, respectively. The results of the theories considered here present great differences. (a) Model II predicts a cross-section smaller than that for the $N = 1$ incoming resonance (figure 2(a)), while I and III predict larger cross-sections than those of figure 2(a). (b) In model III, the peak associated with the $n_p = 2$ vibron becomes bigger than the $n_p = 1$ peak. In models I and III, because the energy of the incoming resonance $\hbar\omega_l = E_3$ is very close to the energy of the outgoing resonance with the $N = 2$ excitonic state $\hbar\omega_s \simeq E_2 + \hbar\omega_p$ (see table 1), a quasi-double-resonant condition takes place in the scattering process. Hence, the Raman cross-section values are strongly dependent on the matrix elements $\langle 3|h^{(n_p)}|2\rangle$, which are maximum for $n_p = 2$, explaining why the $n_p = 2$ peak is greatly enhanced. Moreover, the $n_p = 1$ contribution is dropped because of interference effects between $N = 2$ and $N = 3$ excitonic transitions mediated by the matrix elements $\langle 3|h^{(n_p)}|3\rangle$ and $\langle 3|h^{(n_p)}|2\rangle$. Owing to symmetry, the matrix element $\langle 3|h^{(n_p)}|2\rangle$ vanishes in the framework of the free EHP model and the quasi-double-resonance effect is not observed in figure 2(c). We have also calculated the spectrum in the outgoing resonance with $N = 3$, using models I and III. In this case the double-resonance condition is not fulfilled and the obtained cross-section is similar in both models.

We have finally compared the integral Raman intensity for the $n_p = 1$ vibron of a 20 Å CdS QD and it is shown in figure 3 as a function of the incident photon energy. We have used the same broadening of $\Gamma = 5$ meV for all the excitonic levels. This plot takes up the effects already presented in previous figures over the absolute values of the Raman spectra. The red shift of the resonances due to the attractive electron–hole interaction is shown. Due to the small optical oscillator strength, the intensities corresponding to the incoming and outgoing resonances with the second EHP level in model I are insignificant compared to those of the first and third levels. Model III predicts stronger resonances for the $N = 1$ exciton than model I, a fact explained by the enhancement of its oscillator strength. For all models the $N = 1$ outgoing resonance is stronger than the incoming one, but for the $N = 2$ state the opposite is obtained. The above feature is a general result of the Fröhlich-like interaction in a quantum dot. The $N = 2$ excitonic state has an oscillator strength equal to 1.08, a factor about 30 times larger than for the free EHP (see table 1) and this is the cause of the strong $N = 2$ incoming resonance seen in the plot. The outgoing peak for the $N = 3$ level is smaller in model III than that of the free EHP theory. This is explained by the reduction

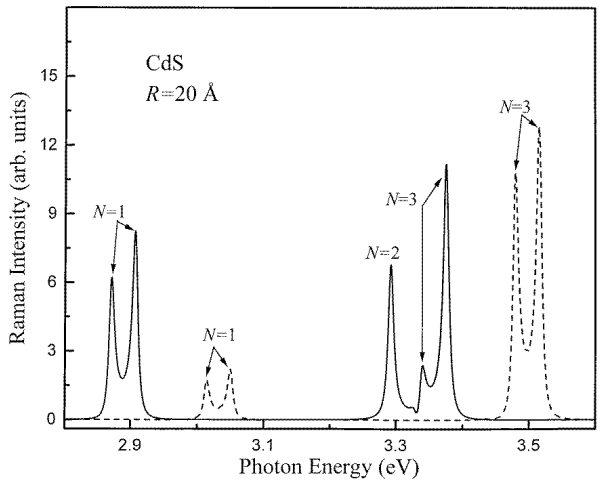


**Figure 3.** Raman intensity for a 20 Å CdS quantum dot, as a function of the incident photon energy, according to model III (solid curve) and I (dashed curve).

of the electron–hole decompensation observed in model III (see figure 1(c)). The intensities calculated according to model II are two orders of magnitude smaller than that of the exciton in the finite-barrier models. This calculation is not presented in figure 3.

## 3. Conclusions

We have studied the influence of excitonic and finite confinement effects on the first-order Raman cross-sections for longitudinal optical vibrons in nanospherical semiconductor quantum dots. We have compared the predictions of three models for the intermediate electronic states: (I) uncorrelated electron–hole pairs with finite dot confinement; (II) excitons completely confined in a spherical box with an effective radius; (III) excitons in a finite confinement barrier. The main conclusion of the present work is that the Raman spectra and the resonance profile absolute values for the Fröhlich-type-interaction Hamiltonian in QDs should be predicted by a theory that takes into consideration both the finite confinement barrier height and electron–hole correlation effects. Even in the strong quantum confinement regime, excitons and the conduction- and valence-band offsets substantially modify the features of the resonant Raman spectra, particularly in the presence of quasi-double resonances.

## Acknowledgments

We would like to thank F Comas and J Tutor for critical readings of the manuscript. Two of us (EM-P and JLP) would like to thank the support of the Secretary of Public Education of Yucatan State, Mexico.

## References

[1] Trallero-Giner C, Debernardi A, Cardona M and Menéndez-Proupin E 1998 *Phys. Rev.* B **57** 4664
[2] Klein M C, Hache F, Ricard D and Flytzanis C 1990 *Phys. Rev.* B **42** 11 123
[3] Scamarcio G, Lugara M and Manno D 1992 *Phys. Rev.* B **45** 13 792
[4] Rodden W S O, Sotomayor-Torres C M and Ironside C N 1995 *Semicond. Sci. Technol.* **10** 807
[5] Krauss T D, Wise F W and Tanner D B 1996 *Phys. Rev. Lett.* **76** 1376
[6] Chamberlain M P, Trallero-Giner C and Cardona M 1995 *Phys. Rev.* B **51** 1680
[7] Menendez E, Trallero-Giner C and Cardona M 1997 *Phys. Status Solidi* b **199** 81
Menendez E, Trallero-Giner C and Cardona M 1997 *Phys. Status Solidi* b **201** 551 (Erratum)
[8] Cardona M 1982 *Light Scattering in Solids II (Topics in Applied Physics 50)* ed M Cardona and G Güntherodt (Heidelberg: Springer) p 19
[9] Trallero-Giner C, Cantarero A and Cardona M 1989 *Phys. Rev.* B **40** 4030
[10] In a quantum dot the concept of phonon as a quasiparticle with translational symmetry is lost, it is then called a vibron.
[11] The matrix elements of the exciton Hamiltonian in a spherical quantum dot can be found in [7]. A misprint has recently been noted in equation (22) where $(-1)^{L+l_h+l'_h}$ must appear in place of $(-1)^{L+l_e+l_h}$.
[12] The oscillator strength values corresponding to model II are: $|f_1|^2 = 1.829$, $|f_2|^2 = 0.129$ and $|f_3|^2 = 4.045$. Note the mistaken values reported in [7].